ARTICLE

ACS chemical biology

Pathway Engineered Enzymatic *de Novo* Purine Nucleotide Synthesis

Heather L. Schultheisz[†], Blair R. Szymczyna[†], Lincoln G. Scott[‡], and James R. Williamson[†,*]

[†]Departments of Molecular Biology and Chemistry, The Skaggs Institute for Chemical Biology, The Scripps Research Institute, 10550 North Torrey Pines Road, MB33, La Jolla, California 92037 and [‡]Cassia, LLC, 4045 Sorrento Valley Boulevard, San Diego, California 92121

ABSTRACT A general method for isotopic labeling of the purine base moiety of nucleotides and RNA has been developed through biochemical pathway engineering *in vitro*. A synthetic scheme was designed and implemented utilizing recombinant enzymes from the pentose phosphate and *de novo* purine synthesis pathways, with regeneration of folate, aspartate, glutamine, ATP, and NADPH cofactors, in a single-pot reaction. Syntheses proceeded quickly and efficiently in comparison to chemical methods with isolated yields up to 66% for ^{13}C-, ^{15}N-enriched ATP and GTP. The scheme is robust and flexible, requiring only serine, NH_4^+, glucose, and CO_2 as stoichiometric precursors in labeled form. Using this approach, U-^{13}C-GTP, U-^{13}C,^{15}N- GTP, $^{13}C_{2,8}$- ATP, and U-^{15}N- GTP were synthesized on a millimole scale, and the utility of the isotope labeling is illustrated in NMR spectra of HIV-2 transactivation region RNA containing $^{13}C_{2,8}$-adenosine and $^{15}N_{1,3,7,9,2}$-guanosine. Pathway engineering *in vitro* permits complex synthetic cascades to be effected, expanding the applicability of enzymatic synthesis.

The expanding field of biocatalysis has emerged as a viable alternative to the chemical synthesis of many compounds. Enzymatic synthesis offers distinct advantages over chemical methods, including reduced reaction time, increased product yield, increased product specificity, reduced cost, and reduced environmental impact (*1–3*). For these reasons, many basic enzymatic syntheses have been adapted for the efficient production of a wide variety of compounds. Examples include vanillin (*4*), amylose (*5*), β-lactam antibiotics (*6*), glycopeptides (*7*), iminocyclitols (*8*), and chiral amino acids (*9*).

Through pathway engineering, it is possible to expand enzymatic synthesis to include a combination of biochemical pathways, increasing the complexity of the accessible targets significantly, yet continuing to maintain the same advantages enjoyed by simple enzymatic syntheses. An elegant example of a complex multistep enzymatic reaction was the synthesis of vitamin B12 from simple precursors, pioneered by A. Ian Scott, using cloned enzymes from different organisms (*10–12*). A bioactive heparan sulfate pentasaccharide was synthesized *in vitro* using eight enzymes from its biosynthetic pathway in the Golgi apparatus with a faster reaction time, increased yield, and using 1/10th of the steps required for total chemical synthesis (*13*). In addition, multistep enzymatic synthesis has recently been used to synthesize enterocin polyketides (*14*). Multistep enzymatic synthesis has also been used for efficient preparative synthesis of ^{13}C- and ^{2}H-labeled ribonucleotides for NMR studies of RNA structure (*15–17*).

Uniformly ^{13}C,^{15}N-labeled nucleotides used in NMR studies of RNA structure and dynamics are obtained from bacteria grown on a minimal medium with $^{15}NH_4Cl$ as the sole nitrogen source and/or $^{13}C_6$-glucose or ^{13}C-methanol as the carbon source (*18–20*). Using this

*Corresponding author, jrwill@scripps.edu.

Received for review March 23, 2008 and accepted June 3, 2008.

Published online August 15, 2008

10.1021/cb800066p CCC: $40.75

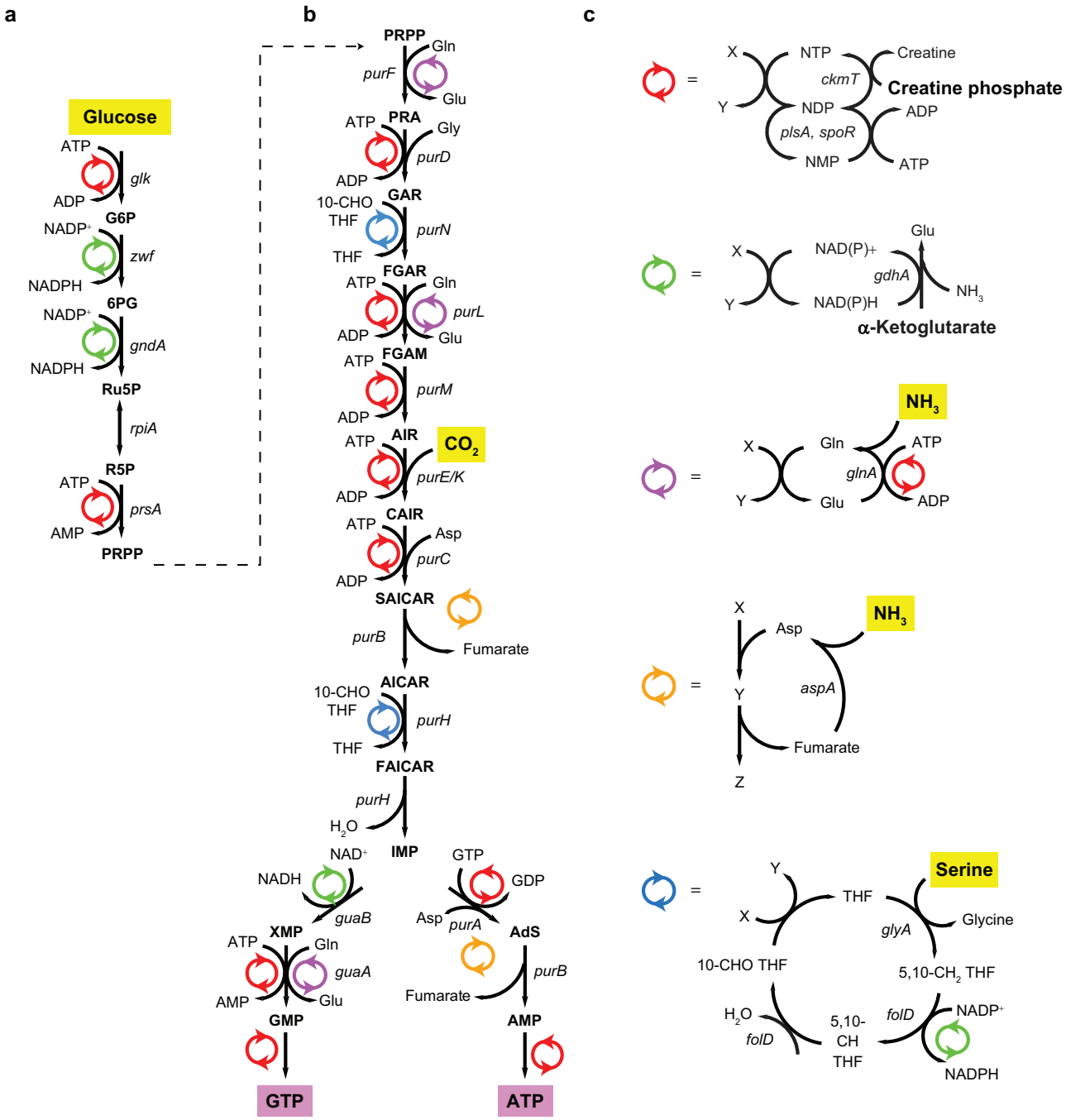
a
Glucose
ATP
ADP
glk
G6P
NADP+
NADPH
zwf
6PG
NADP+
NADPH
gndA
Ru5P
rpiA
R5P
ATP
AMP
prsA
PRPP
b
PRPP
Gln
purF
Glu
ATP
PRA
Gly
purD
ADP
GAR
10-CHO THF
purN
THF
FGAR
ATP
Gln
purL
ADP
Glu
ATP
FGAM
purM
ADP
ATP
AIR
CO2
purE/K
ADP
ATP
CAIR
Asp
purC
ADP
SAICAR
purB
Fumarate
AICAR
10-CHO THF
purH
THF
FAICAR
purH
H2O
IMP
NAD+
NADH
guaB
XMP
ATP
Gln
guaA
AMP
Glu
GMP
GTP
GTP
GDP
Asp
purA
AdS
purB
Fumarate
AMP
ATP
c
=
X
Y
NTP
Creatine
ckmT
Creatine phosphate
NDP
ADP
plsA, spoR
NMP
ATP
=
X
Y
NAD(P)+
Glu
gdhA
NH3
NAD(P)H
α-Ketoglutarate
=
X
Y
Gln
ATP
NH3
glnA
Glu
ADP
=
X
Asp
NH3
Y
aspA
Fumarate
Z
=
Y
X
THF
Serine
glyA
Glycine
10-CHO THF
5,10-CH2 THF
H2O
folD
5,10-
CH
THF
folD
NADP+
NADPH

Figure 1. Scheme for enzymatic synthesis of purine nucleotides. a) Conversion of glucose to PRPP. Glucose and ATP are converted to glucose-6-phosphate (G6P) by the action of glucokinase (*glk*) with the production of ADP. G6P and $NADP^+$ are converted to 6-phosphogluconate (6PG) by glucose-6-phosphate dehydrogenase (*zwf*) with the production of NADPH. 6PG and $NADP^+$ are converted to ribulose-5-phosphate (Ru5P) by the action of 6-phosphogluconate dehydrogenase (*gndA*) with the production of NADPH. Phosphoriboisomerase (*rpiA*) interconverts Ru5P and ribose-5-phosphate (R5P). R5P and ATP are converted to phosphoribose-pyrophosphate (PRPP) by the action of PRPP synthase (*prsA*) with the production of AMP. b) Conversion of PRPP to ATP or GTP. PRPP and glutamine are converted to phosphoribose-amine (PRA) by the action of amidophosphoribosyl-transferase (*purF*) with the production of glutamine. PRA, glycine, and ATP are converted to phosphoribosyl-glycinamide (GAR) by the action of phosphoribosylamine-glycine ligase (*purD*) with the production of ADP. GAR and 10-formyl-tetrahydrofolate are converted to phosphoribosyl-formylglycinamide (FGAR) by the action of phosphoribosyl-glycine amide formyltransferase (*purN*) with the production of tetrahydrofolate (THF). FGAR, glutamine, and ATP are converted to phosphoribosyl-formylglycinamidine (FGAM) by the action of FGAM synthase (*purL*) with the production of glutamate and ADP. FGAM and ATP are converted to phosphoribosyl-aminoimidazole (AIR) by phosphoribosyl-formyl glycinamidine cyclo-ligase (*purM*) with the production of ADP. AIR, CO_2, and ATP (*47*) are converted to phosphoribosyl-amino-carboxy-imidazole (CAIR) by the action of phosphoribosyl-amino-imidazole carboxylase (*purE, purK*) with the production of ADP. CAIR, aspartate, and ATP are converted to phosphoribosyl-amino-succinocarboxamide-imidazole (SAICAR) by phosphoriobsyl-aminoimidazole-succino-carboxamide synthase (*purC*) with the production of ADP. SAICAR is converted to phosphoribosyl-amino-imidazole carboxamide (AICAR) by adenylosuccinate lyase (*purB*) with the production of fumarate. AICAR and 10-formyl-THF are converted to phosphoribosyl-formylamido-imidazole carboxamide (FAICAR) by the action of phophoribosylamino-imidazole-carboxamide formyltransferase (*purH*) with the production of THF. FAICAR is converted to inosine monophosphate (IMP) by IMP cyclohydrolase (*purH*) with the production of H_2O. For ATP: IMP and GTP are converted to adenylosuccinate (AdS) by adenylosuccinate synthase (*purA*) with the production of GDP. AdS is converted to AMP by the action of *purB* with the production of fumarate. For GTP: IMP and NAD^+ are converted to xanthosine monophosphate (XMP) by the action of IMP dehydrogenase (*guaB*) with the production of NADH. XMP, glutamine, and ATP are converted to GMP by the action of GMP synthase (*guaA*) with the production of AMP and glutamate. c) Cofactor regeneration schemes. *NTP regeneration (red)*. AMP and ATP are converted to ADP by the action of adenylate kinase (*plsA*). GMP and ATP are converted to GDP by the action of guanylate kinase (*spoR*) with the production of ADP. NDPs and creatine phosphate are converted to NTPs by the action of creatine phosphokinase (*ckmT*) with the production of creatine. *NAD regeneration (green)*. NAD(P)H, α-ketoglutarate (α-KG), and NH_3 are converted to $NAD(P)^+$ by the action of glutamate dehydrogenase (*gdhA*) with the production of glutamate. *Glutamine recycling (purple)*. Glutamate, ATP, and NH_3 are converted to glutamine by the action of glutamine synthase (*glnA*) with the production of ADP. Aspartate recycling *(orange)*. Fumarate and NH_3 are converted to aspartate by the action of aspartate ammonia-lyase (*aspA*). *Folate regeneration (blue)*. THF and serine are converted to 5,10-CH_2-THF by the action of glycine hydroxymethyl-transferase (*glyA*) with the production of glycine. 5,10-CH_2-THF and $NADP^+$ are converted to 5,10-CH-THF by the action of methylene-THF dehydrogenase (*folD*) with the production of NADPH. 5,10-CH-THF is converted to 10-CHO (formyl) THF by the action of methenyl-THF cyclohydrolase (*folD*) with the production of H_2O.

method, labeled nucleotides can be produced economically in gram quantities, but specific isotope labeling patterns are not possible. Specific incorporation of ^{13}C,^{15}N can be used to reduce spectral crowding, as a spectral filter, or to simplify the dipolar network for relaxation studies (*16, 21–23*).

Selective incorporation of isotope labels into nucleotides can be effected by chemical and/or enzymatic synthesis. Using ^{13}C,^{2}H-labeled glucose and unlabeled bases, efficient enzymatic synthesis of a variety of specific ribose-labeled nucleotides was carried out, facilitating the study of RNA molecules of increasing size (*15–17, 24*). Specific labeling of the ribose moiety permits assignment of sugar−sugar and intermolecular NOE correlations by reducing ambiguity and crowding of the spectra. The two most important protons for NMR structural analysis, H1′ and H2′, can be selectively observed, and the variety of available labeling patterns for the glucose starting material provides a great degree of flexibility for labeling of the ribose moiety (*17*).

The next logical step is to expand specific isotope labeling to the base. The base moiety of RNA and DNA molecules contains key structural information in local interactions including hydrogen bonding, protonation, ligand interactions, and stacking (*22, 23, 25*). Chemical synthesis has been the main source for specific ^{13}C,^{15}N base labeling to date (*26, 27*). Several groups have incorporated ^{13}C,^{15}N at specific positions in the base of purine nucleotides using a combination of chemical and enzymatic synthesis. Starting from 4,5,6-triaminopyrimidine or 2,4,5,6-tetraaminopyrimidine, $^{13}C_8$-labeled adenine or 2,6-diaminopurine were chemically synthesized, followed by combined chemical and enzymatic conversion to ATP or GTP, with overall yields of 37% and 29%, respectively (*23*). Similarly, starting from imidazole-4,5-dicarboxylic acid, hypoxanthine and 2-methylthio-hypoxanthine were chemically synthesized, followed by a combination of enzymatic and chemical synthesis to introduce specific labels at $^{13}C_2$–$^{15}N_{1,3,amino}$, giving 35% overall yield for adenosine and

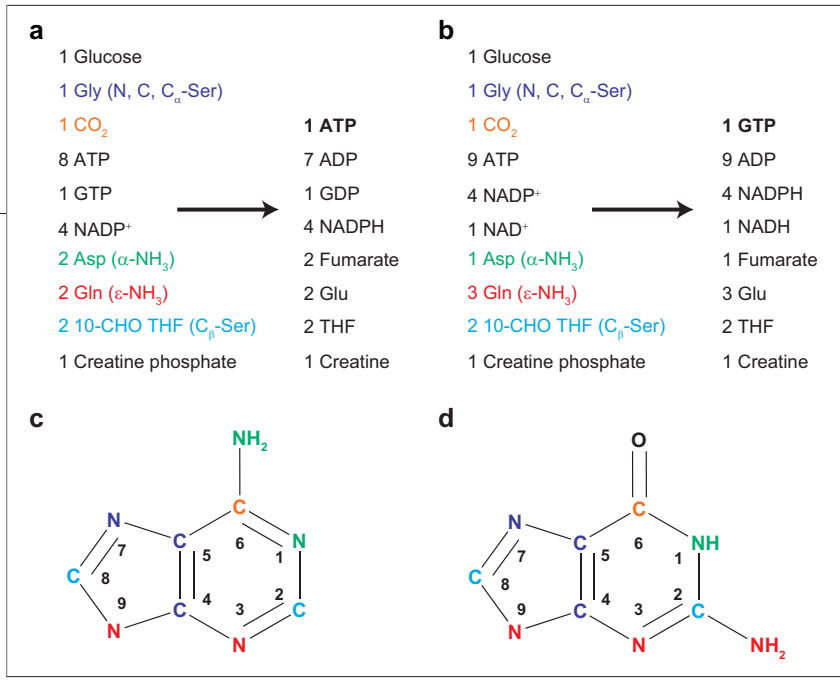

Figure 2. Substrates and products of biosynthesis for a) ATP and b) GTP. Metabolic origin of purine atoms for c) adenine and d) guanine. The substrates and the metabolic source for each purine atom are color-coded: glycine (blue), CO_2 (orange), aspartate (green), glutamine (red), 10-formyl-THF (cyan).

40% for guanosine (*28*). Starting from inosine, $^{13}C_2{}^{15}N_{1,amino}$-guanosine was synthesized in 32% overall yield (*29*). The 2-amino group of GMP has also been labeled with ^{15}N through enzymatic interconversion of NMPs (*30*). These synthetic schemes and starting materials vary widely in implementation and difficulty depending on the desired nucleotide and labeling pattern. In general, uniformly or specifically labeled purine bases are not commercially available, and chemical synthesis of labeled purines is complex (*22, 26, 27, 31*). A general, flexible, and efficient enzymatic synthesis of base-labeled purine nucleotides would have many applications in biochemical and biophysical studies of nucleic acid structure and function.

In the present work, *de novo* purine biosynthesis is coupled with phosphoribosyl-pyrophosphate (PRPP) synthesis to effect a total enzymatic synthesis of the purine nucleotides ATP and GTP. The synthesis is carried out with the precursors glucose, glutamine, serine, ammonia, and CO_2 that are available in a variety of isotopically labeled forms. A total of 28 biosynthetic enzymes were used for the efficient synthesis of ATP and GTP with yields of up to 66% in a single-pot reaction. The reaction design relies heavily on NTP and NAD(P)H cofactor regeneration schemes (*32, 33*), and in addition, novel recycling reactions for folate, fumarate, and glutamine cofactor pools were implemented. As a result of the flexibility afforded by selection of labeled starting materials, a wide variety of purine isotope labeling patterns are possible. Using this approach, U-^{13}C- GTP, U-^{13}C,^{15}N-GTP, $^{13}C_{2,8}$- ATP and U-^{15}N- GTP were synthesized on a millimolar scale, and the utility of these labeled nucleotides is illustrated in NMR spectra of an RNA oligomer containing $^{13}C_{2,8}$-adenosine and $^{15}N_{1,3,7,9,2}$-guanosine.

RESULTS AND DISCUSSION

Design of the Enzymatic Synthesis. The well-established metabolic pathway for *de novo* purine biosynthesis is outlined in Figure 1, panels a and b. Enzymes of the pentose phosphate pathway convert glucose to PRPP, which enters into the linear cascade of reactions that assemble the purine ring to produce IMP, which is the precursor for both ATP and GTP. The net reaction for biosynthesis of ATP and GTP is shown in Figure 2, panels a and b, including the precursor molecules as well as the numerous cofactors that are consumed in the reaction cascade. The atoms in the purine ring are metabolically derived from glycine, CO_2, aspartate, glutamine, and 10-formyl THF as shown in Figure 2, panels c and d, and this set of precursors defines the possible isotope labeling patterns that can be achieved using *in vitro* biosynthesis. The goal of the present work is to recapitulate the *de novo* purine biosynthesis cascade *in vitro*, using purified recombinant enzymes and a defined set of labeled precursors to generate specifically isotopically labeled nucleotides.

For efficient enzymatic synthesis *in vitro*, there are three major considerations. First, isotopically labeled amino acids are expensive starting materials. ^{13}C-labeled 10-formyl THF is not commercially available, and it is necessary to generate these labeled precursor components *in situ*. Second, the numerous ATP and GTP equivalents required cannot be supplied in stoichiometric amounts to avoid isotopic dilution of the desired nucleotide products, and it is essential to employ enzymatic cofactor regeneration schemes. Third, it is important to provide a driving force for the overall reaction to ensure high yields of the desired labeled ATP and GTP. All of these considerations can be taken into account to design and effect an efficient and cost-effective enzymatic synthesis scheme.

The overall strategy for *de novo* purine nucleotide synthesis builds on the previously implemented syntheses of nucleotides from glucose and bases, *via* the PRPP intermediate, as shown in Figure 1, panel a (*15–17*). The cofactor recycling schemes for regeneration of NTPs

from NMPs or NDPs and regeneration of NAD(P)$^+$ from NAD(P)H are well-established (*34, 35*), as shown in Figure 1, panel c. Creatine phosphate is a suitable phosphate source for rephosphorylation of NDPs by the action of creatine kinase. NAD(P)$^+$ regeneration is accomplished by the action of glutamate dehydrogenase on α-ketoglutarate and ammonia, to produce glutamate. Because neither glutamate nor creatine directly supply labeled atoms to the final product, these reagents may be used in excess to provide a driving force for the overall reaction.

During the ATP synthesis, the enzymes continue to utilize and regenerate labeled ATP as it is produced. To initiate the reaction, it is necessary to add a catalytic amount of unlabeled ATP (1%). In addition, a catalytic amount of unlabeled GTP (1%) is added as a required cofactor for conversion of IMP to adenylosuccinate by adenylosuccinate synthase (*purA*). The labeled ATP that is synthesized will unavoidably contain 1% unlabeled ATP and 1% unlabeled GTP, but for preparation of labeled RNAs for NMR studies, this has a negligible effect on the overall labeling.

GTP synthesis is equally dependent on ATP, but addition of 1% catalytic ATP is not sufficient to initiate the reaction. Although increasing the ATP concentration is effective, the subsequent separation of labeled GTP from unlabeled ATP involves a difficult chromatography step. Fortunately, the ATP requirement for the GTP synthesis reaction can be met by the addition of 10% dATP, which is readily separated from the final product GTP during the boronate affinity chromatography step. Several enzymes including hexokinase, PRPP synthase (*prsA*), both monophosphate kinases (*plsA, spoR*), and glutamine synthase (*glnA*) utilize dATP with slightly lower efficiency than ATP. However, GMP synthase (*guaA*) will not accept dATP as a substrate, and it is still necessary to add a catalytic amount of ATP (1%) during GTP synthesis in the presence of dATP. Both ATP and dATP are regenerated by creatine phosphokinase, efficiently fueling the GTP reaction. In this way, dATP provides the critical phosphate source in the GTP synthesis reaction without contributing to isotopic dilution or mixing of the nucleotide pool.

To implement the purine biosynthesis cascade, shown in Figure 1, panel b, several additional cofactor recycling schemes needed to be developed. Four of the nitrogen atoms in ATP or GTP are derived from the α-amino group of aspartate or the ε-amino group of glutamine, and both of these positions can be enzymatically labeled, *in situ* from ^{15}N-ammonium ions, as shown in Figure 1 c. Generation of ε-^{15}N-glutamine can be accomplished *in situ* from glutamate using glutamine synthase, while generation of α-^{15}N-aspartate can be accomplished *in situ* from fumarate using aspartate-ammonia lyase (*aspA*). Glutamine is used in three reactions for the incorporation of the purine N3 and N9 atoms and the guanine N2 atom, releasing glutamate, which can be recycled to form ε-^{15}N-glutamine by the action of *glnA*, as shown in Figure 1, panels b and c. Aspartate is used in two similar two-step reaction sequences for incorporation of the purine N1 atom and the adenine N6 atom, both reactions releasing fumarate, which can be recycled to form α-^{15}N-aspartate by the action of *aspA*, as shown in Figure 1, panels b and c. In this reaction scheme, glutamate is generated *in situ* from recycling of NAD(P)H, and only catalytic amounts of fumarate must be added. The action of *glnA* and *aspA* effectively recycles the pools of glutamine and aspartate cofactors.

The purine C2 and C8 positions are derived from 10-formyl-THF; however, ^{13}C-labeled folates are not commercially available. It is possible to generate ^{13}C-10-formyl-THF *in situ* and recycle catalytic amounts of tetrahydrofolate (THF) as a cofactor, using the scheme shown in Figure 1, panel c. The β-carbon of serine is incorporated into 10-formyl-THF by the sequential action of serine hydroxymethyl transferase (*glyA*) and the multifunctional enzyme *folD*, which provides for efficient recycling of the folate cofactor pool during nucleotide synthesis.

The recycling schemes shown in Figure 1, panel c for the NTP, NAD(P)H, glutamate, fumarate, and folate pools make the overall synthesis of ATP and GTP, shown in Figure 1, panels a and b, streamlined and efficient. Almost every step of the linear sequence from glucose to ATP/GTP is facilitated by recycling of one of these cofactor pools. The net reaction for the enzymatic scheme shown in Figure 1, panels a and b, including the effects of cofactor recycling, is given in Figure 3, panels a and b for ATP and GTP synthesis, respectively. The set of starting materials for the overall reaction shown in Figure 2, panels a and b is simplified to a small number of reagents that fall into three classes. First, there is a set of stoichiometric reagents that are ultimately incorporated into the nucleotide, which includes glucose, CO_2, ammonia, and serine. Second, the large number of phos-

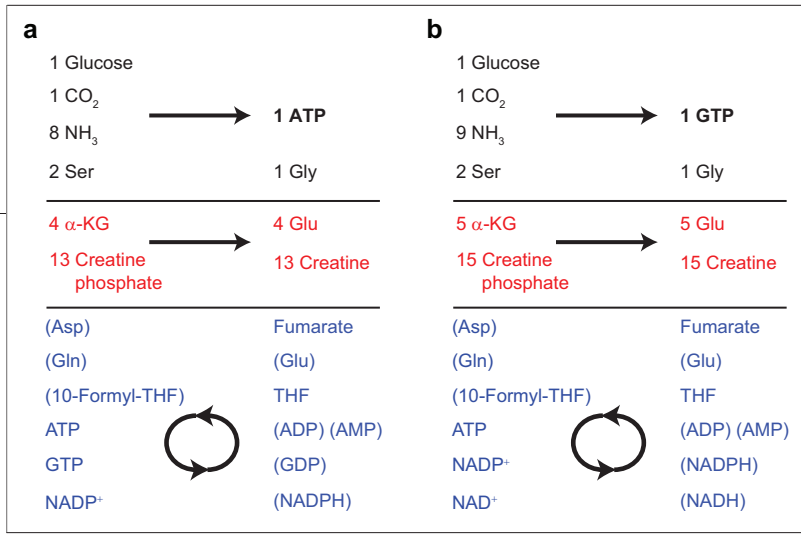

Figure 3. Pathway engineered synthesis scheme for a) ATP and b) GTP. Reagents are color coded: stoichiometric isotopically labeled reagents (black), phosphate and oxidizing equivalents as the driving force (red), and recycled cofactors (blue). Cofactors are added in catalytic amounts, and intermediates that are generated *in situ* are shown in parentheses.

phate and reducing equivalents are supplied with creatine phosphate and α-ketoglutarate, respectively. These two reagents are supplied in excess to provide a driving force that fuels the overall reactions. Third, a set of cofactors is supplied in catalytic amounts. The complex cascade of reactions in Figure 1, panels a and b is effectively reduced to a net transformation of glucose, CO_2, ammonia, and serine into ATP/GTP, with one byproduct molecule of glycine in addition to the creatine and glutamate byproducts from cofactor regeneration.

In the net reaction, carbons of the purine ring originate from only serine (C2,C4,C5,C8) and CO_2 (C6), while the nitrogens of the purine ring are derived from serine (N7) and NH_4^+ ions (N1,N2,N3,N6,N9). There is a tremendous flexibility available generating specific labeling patterns by the suitable choice of labeled starting materials. As a result of the availability of specifically labeled serine, all of the purine base carbons can be separately labeled except for C2 and C8. For nitrogen, it is possible to separate the N3, N9 from N1 by using labeled aspartate directly, and N7 is separately labeled from serine.

There is one restriction placed on possible labeling patterns due to the production of CO_2 by decarboxylation of 6-phosphogluconate to ribulose-5-phosphate during PRPP generation. This step effectively couples the isotope composition of the C1 of glucose to C6 in the purine base *via* the CO_2 pool, and care must be taken to avoid isotopic scrambling or isotopic dilution due to atmospheric CO_2 in certain cases. If ^{13}C-ribose and ^{13}C6-purine labeling are both desired, then degassing and inert atmosphere are sufficient to prevent isotopic dilution (see Supplementary Figure 9). If ^{13}C6 purine labeling is desired without ribose labeling, then PRPP can be generated enzymatically directly from unlabeled ribose (*15*). If ^{13}C-ribose labeling from ^{13}C-glucose is desired without ^{13}C6-purine labeling, then an excess of $^{12}CO_2$ can be supplied. For synthesis of two different labeled nucleotides, ^{13}C labeling of the base and the ribose moieties was successfully combined.

Implementation of the Enzymatic Synthesis. There are 28 enzymes required to implement the *de novo* enzymatic synthesis of GTP and ATP shown in Figure 1, and few of these are commercially available. Given our previous success with *E. coli* phosphoribosyltransferases (*15, 16, 36, 37*) and the extensive characterization of the purine biosynthesis pathway (*38*), the entire set of *E. coli* enzymes for the reactions in Figure 1 was cloned, expressed, and purified. Many of the intermediates in Figure 1 are not commercially available, and it was not possible to perform activity assays on many of the expressed enzymes. In these cases, the value for the specific activity was assumed to be 1 U mg^{-1}. Fortunately, all of the selected enzymes were catalytically active, and *de novo* synthesis of ATP was observed in the first model reaction. The reactions described below were not extensively optimized, and it appears that this enzymatic synthesis scheme is very stable and robust. To illustrate the flexibility and utility of the pathway engineered

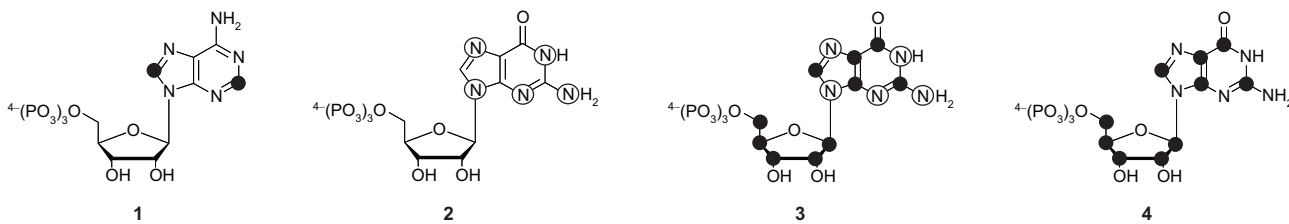

Figure 4. Molecular structures of compounds synthesized: (1) ^{13}C-$C_{2,8}$-ATP, (2) U-^{15}N-GTP, (3) U-^{13}C,^{15}N-GTP, (4) U-^{13}C-GTP. ^{13}C labels are indicated by black circles, and ^{15}N labels are indicated by open circles.

TABLE 1. Complete list of enzymes for *de novo* enzymatic synthesis of ATP and GTP[a]

Enzyme	Gene	EC	Source[b]	1	2	3	4
Hexokinase	*hxk1/2*	2.7.1.1	BY	5.6 U	5.6 U		
Glucokinase	*glk*	2.7.1.2	RE			2.4 U	2.4 U
Glucose-6-phosphate dehydrogenase	*zwf1*	1.1.1.49	BY	6.2 U	6.35 U		
Glucose-6-phosphate dehydrogenase	*zwf*	1.1.1.49	RE			2.6 U	2.6 U
Phosphogluconate dehydrogenase	*gndA*	1.1.1.44	RE	6.8 U	6.85 U	2.9 U	2.9 U
Ribose-5-phosphate isomerase	*rpiA*	5.3.1.6	RE	7.5 U	7.5 U	3.2 U	3.2 U
Ribose-phosphate diphosphate kinase	*prsA*	2.7.6.1	RE	8.2 U	8.2 U	3.5 U	3.5 U
Amidophosphoribosyl-transferase	*purF*	2.4.2.14	RE	10.5 mg	15.2 mg	4.0 mg	4.0 mg
Phosphoribosylamine-glycine ligase	*purD*	6.3.4.13	RE	14.4 mg	12.5 mg	4.3 mg	4.3 mg
Phosphoribosylglycinamide formyltransferase	*purN*	2.1.2.2	RE	4.6 mg	7.5 mg	4.7 mg	4.7 mg
Phosphoribosylformylglycinamidine synthase	*purL*	6.3.5.3	RE	25.6 mg	25.2 mg	5.4 mg	5.4 mg
Phosphoribosylformylglycinamidine cyclo-ligase	*purM*	6.3.3.1	RE	11.7 mg	7.8 mg	5.7 mg	5.7 mg
Phosphoribosylamino-imidazole carboxylase (catalytic subunit)	*purE*	4.1.1.21	RE	18.7 mg	35.4 mg	6.5 mg	6.5 mg
Phosphoribosylamino-imidazole carboxylase (ATPase subunit)	*purK*	4.1.1.21	RE	6.0 mg	8.5 mg	6.2 mg	6.2 mg
Phosphoribosylamino-imidazole-succinocarboxamide synthase	*purC*	6.3.2.6	RE	3.4 mg	6.9 mg	7.0 mg	7.0 mg
Adenylosuccinate lyase	*purB*	4.3.2.2	RE	56 U	28 U	10 U	10 U
Phosphoribosylamino-imidazole-carboxamide formyltransferase	*purH*	2.1.2.3	RE	14 mg	31 mg	18 mg	18 mg
Inosine-monophosphate cyclohydrolase	*purH*	3.5.4.10	RE				
Adenylosuccinate synthase	*purA*	6.3.4.4	RE	10 U			
Inosine-monophosphate dehydrogenase	*guaB*	1.1.1.205	RE		25.4 U	15 U	15 U
Guanosine-monophosphate synthase	*guaA*	6.3.5.2	RE		25.8 U	16.5 U	16.5 U
Adenylate kinase	*ak5*	2.7.4.3	CM	200 U			
Adenylate kinase	*plsA*	2.7.4.3	RE		47 U	9 U	9 U
Creatine phosphokinase	*ckmT*	2.7.3.2	RM	250 U	118 U		
Creatine phosphokinase	*ckmT*	2.7.3.2	RE			125 U	125 U
Guanylate kinase	*spoR*	2.7.4.8	RE	1 U	55 U	18 U	18 U
Glycine hydroxymethyltransferase	*glyA*	2.1.2.1	RE	22.5 mg	25 mg	20.2 mg	20.2 mg
Methylene-tetrahydrofolate dehydrogenase	*folD*	1.5.1.5	RE	10.5 mg	23.4 mg	20.2 mg	20.2 mg
Methenyl-tetrahydrofolate cyclohydrolase	*folD*	3.5.4.9	RE				
Aspartate ammonia-lyase	*aspA*	4.3.1.1	RE	92 U	32 U	20 U	20 U
Glutamate dehydrogenase	*glud1*	1.4.1.3	BL	94 U	141 U		
Glutamate dehydrogenase	*gdhA*	1.4.1.4	RE			39 U	39 U
Glutamine synthase	*glnA*	6.3.1.2	RE			38 U	
Inorganic diphosphatase	*ppa*	3.6.1.1	RE	23.4 U	24 U	26 U	26 U

[a]Amounts of each enzyme used for synthesis of compounds **1**–**4** in Figure 4 is provided as either Units of enzyme or mg of enzyme. [b]RE = recombinant from *E. coli*, BY = baker's yeast, CM = chicken muscle, RM = rabbit muscle, BL = bovine liver.

nucleotide synthesis, four different labeled nucleotides were synthesized, as shown in Figure 4.

Synthesis of $^{13}C_{2,8}$-ATP. A 1.2 mmol scale ATP synthesis was performed with labeling of the C8 and C2 of adenine using β-^{13}C-serine. The labeled serine was combined with stoichiometric substrates (glucose, NH_4Cl, glutamine, $KHCO_3$), fuel reagents (α-ketoglutarate, creatine phosphate), catalytic cofactors (ATP, GTP, $NADP^+$, fumarate, THF), and the 23 enzymes listed in Table 1 (**1**) in a 120-mL buffered reaction incubated at 37 °C. ATP formation was monitored by HPLC over the course of 2 days, when the reaction ceased to progress. Affinity purification afforded a 57% isolated yield of $^{13}C_{2,8}$-ATP, based on input glucose, which compares favorably to yields for ATP synthesis from adenine and glucose (*16, 17*).

Synthesis of U-^{15}N-GTP. A 1.2 mmol scale GTP synthesis was performed to produce uniform ^{15}N-labeling by combining stoichiometric substrates (glucose, $^{15}NH_4Cl$, $^{15}N_\varepsilon$-glutamine, serine, $KHCO_3$), fuel reagents (α-ketoglutarate, creatine phosphate), catalytic cofactors (ATP, dATP, $NADP^+$, fumarate, THF), and the 24 enzymes listed in Table 1 (**2**) in a 120-mL buffered reaction incubated at 37 °C. GTP formation was monitored by HPLC; after approximately 2 days, the reaction ceased to progress, and U-^{15}N-GTP was obtained in 24% yield after purification. The lower yield is likely due to the instability of one or more of the *de novo* purine biosynthesis enzymes. Without commercially available substrates, it is difficult to determine which enzymes suffered loss of activity over the months that elapsed after the initial synthesis of $^{13}C_{2,8}$-ATP. In earlier pilot-scale models, the GTP synthesis proceeded similarly to the ATP synthesis, and subsequent syntheses with fresh enzymes were more efficient.

Synthesis of U-^{13}C-^{15}N-GTP. A 0.5 mmol scale GTP synthesis was carried out starting with stoichiometric labeled reagents (^{13}C-glucose, $^{15}NH_4Cl$, ^{13}C/^{15}N-serine, $NaH^{13}CO_3$), fuel reagents, and catalytic cofactors as described above. Fresh preparations of the 27 recombinant enzymes listed in Table 1 (**3**) were used, and the enzymatic recycling of glutamine was included to permit use of $^{15}NH_4Cl$ as the primary nitrogen source. Increased consumption of creatine phosphate was observed as a result of the addition of (d)ATP-dependent *glnA*. The reaction was monitored by HPLC, and after 40 h it was complete. An isolated yield of 42% U-^{13}C-^{15}N-GTP was obtained after purification.

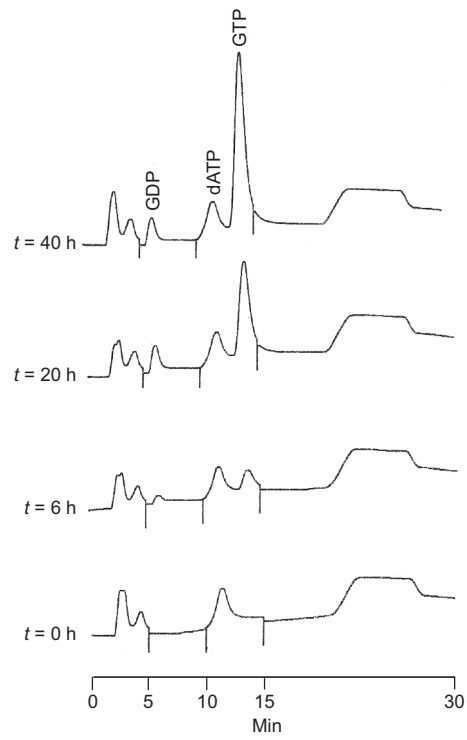

Figure 5. HPLC chromatograms showing the timecourse of the U-^{13}C-GTP-forming reaction. The early eluting peaks are from the NAD(P)$^+$ and THF cofactors.

Synthesis of U-^{13}C-GTP. A 0.5 mmol scale GTP synthesis was performed starting with stoichiometric reagents (^{13}C-glucose, NH_4Cl, glutamine, ^{13}C-serine, $NaH^{13}CO_3$), fuel reagents, and recycled cofactors as described above. The 26 recombinant enzymes listed in Table 1 (**4**) were added, and the time course of the reaction was monitored by HPLC over the course of 40 h, as shown in Figure 5. An isolated yield of 66% U-^{13}C-GTP was obtained after purification.

Incorporation of Labeled Nucleotides into RNA. To demonstrate the utility of the labeled nucleotides, HIV-2 transactivation region (TAR) RNA was transcribed *in vitro* using unlabeled CTP and UTP and the U-^{15}N-GTP and $^{13}C_{2,8}$-ATP prepared as described above. The H2 and H8 resonances of adenine can be selectively observed in a ^{1}H,^{13}C HSQC spectrum, shown in Figure 6, panel b. Similarly, correlations between the guanine H8 and N7 atoms are selectively observed in the ^{1}H,^{15}N-HSQC spectrum shown in Figure 6, panels c and d. NOESY spectra were also acquired on the RNA, show-

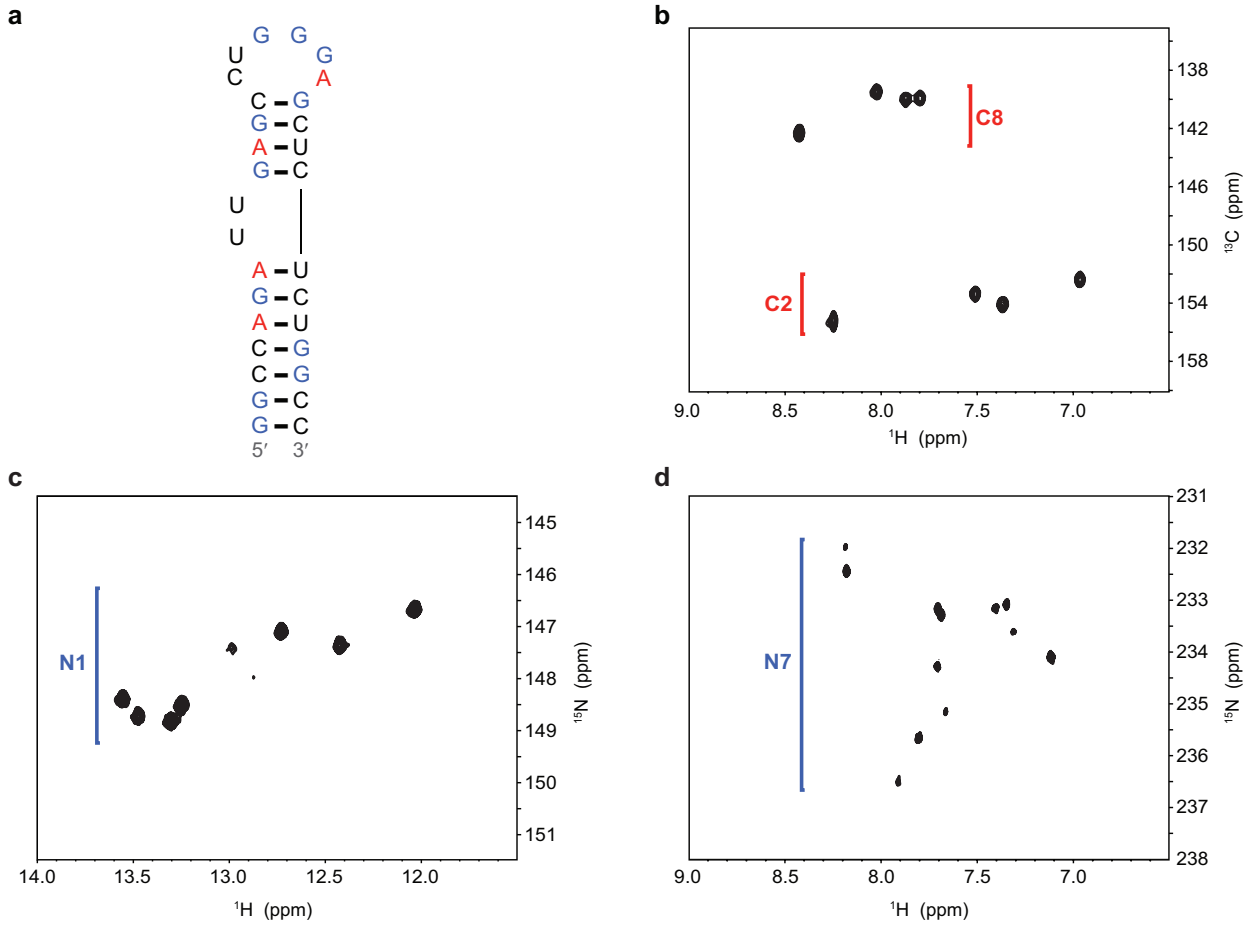

Figure 6. $^{1}H-^{15}N$ and $^{1}H-^{13}C$ HSQC correlation spectra at 10 °C for TAR RNA uniformly labeled with ^{15}N-labeled guanosine and adenosine labeled with ^{13}C at positions 2 and 8. a) Sequence of the partially labeled TAR-2 construct. b) One-bond correlations between protons and the labeled carbons in the four adenosine bases. c) One-bond correlations between N1 and the eight hydrogen-bonded imino protons. d) Two-bond correlations between the nonexchangeable H8 proton and the N7 atom.

ing selection for specific proton interactions edited by both the ^{15}N and ^{13}C labels shown in Figures 7 and 8, respectively. This labeling pattern imparts the ability to discern specific base interactions and reduce crowding and overlap seen with unlabeled or uniformly labeled samples.

Conclusion. Using simple starting materials that are readily available in isotopic form, both ATP and GTP can be synthesized *de novo* with a variety of isotopic labeling patterns in yields comparable to those of syntheses with a preformed base. Enzymes originating from different biochemical pathways combined with several cofactor regeneration schemes, including a portion of the folate cycle, worked together elegantly in one pot. This approach provides isotopically labeled nucleotides in efficiency superior to that of both chemical synthesis and biomass extraction. With all of these factors included in our pathway design, we have been successful in implementing *de novo* purine biosynthesis *in vitro* to effect a flexible, robust, and cost-effective synthesis of isotopically labeled purine nucleotides. It should be possible to extend this approach to labeled pyrimidine nucleotide synthesis, as well as synthesis of labeled amino acids and cofactors.

Through pathway engineering, the efficiency and elegance of synthesis in nature can be employed *in vitro*.

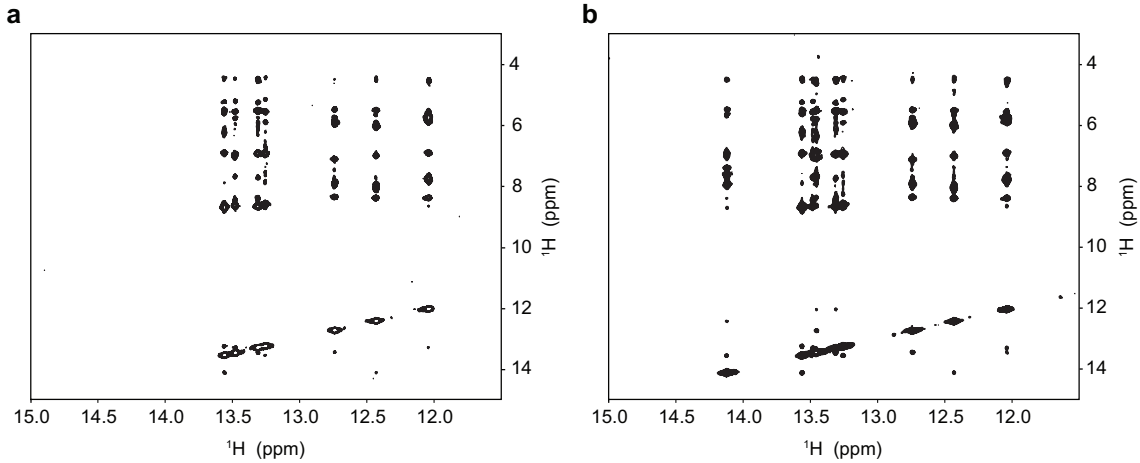

Figure 7. Spectra of TAR RNA. a) ^{15}N-edited and b) homonuclear NOESY (T_{mix} = 250 ms) spectra of TAR RNA uniformly labeled with ^{15}N-labeled guanosine and adenosine labeled with ^{13}C at positions 2 and 8.

The interdependence of biosynthetic pathways, the complex flux of metabolites, and the cost and limited availability of biosynthetic precursors provide significant challenges when excising a pathway from its cellular context. Selective fusion of metabolic pathways, regeneration of expensive cofactors, and *in situ* labeling can be accomplished while simultaneously providing a driving force for the desired synthesis from a simple set of starting materials. On the basis of all of these factors and the complexity of the purine nucleotide synthetic scheme, we suggest that this work expands the limits of the capabilities for *in vitro* enzymatic synthesis and the scope of its applicability for synthesis of high value biochemicals.

METHODS

Materials. Chemicals were purchased from Sigma. L-Serine ($^{13}C_3$, 99%), L-serine ($^{13}C_{1,2,3}$, 98%), L-serine (^{15}N, 98%), L-serine (^{15}N, 98%; $^{13}C_{1,2,3}$, 98%), L-glutamine ($^{15}N_{amide}$, >98%), $NaHCO_3$ (^{13}C, 99%), D-glucose ($^{13}C_{1,2,3,4,5,6}$, 99%), and NH_4Cl (^{15}N, 99%) were purchased from Cambridge Isotope Laboratories. Hexokinase from baker's yeast, glucose-6-phosphate dehydrogenase from baker's yeast, creatine phosphokinase from rabbit muscle, adenylate kinase from chicken muscle, and glutamic dehydrogenase from bovine liver were purchased from Sigma. *PrsA* prepared as described previously was used for synthesis of compounds **1** and **2** (*39*), and the new recombinant *prsA* was used for synthesis of compounds **3** and **4**.

Enzyme Cloning. The genes for all recombinant *E. coli* enzymes in Table 1 were cloned from the *E. coli* K12 MRE600 genome, based on the reported gene sequences in Genbank using standard procedures. Each gene was amplified from genomic DNA using PCR with gene-specific primers containing compatible restriction sites of either *Bam*HI, *Hin*dIII, *Eco*RI, or XhoI for cloning into pET22-HT (derived from pET22b, Novagen) encoding a N-terminal hexahistidine tag. *E. coli* strain DH5α was used for cloning and plasmid maintenance. All constructs were verified by DNA sequencing. Rabbit muscle creatine phosphokinase was amplified from pET17b-RMCK, a gift from George Kenyon, University of Michigan (*40*). A single point mutation, Y397F, was introduced to glutamine synthase, enhancing specific activity as previously shown (*41*).

Enzyme Purification. Plasmids were transformed into *E. coli* BL21(DE3) cells for protein overexpression. Overnight 5-mL cultures in LB with 100 μg mL^{-1} ampicillin were diluted 100-fold and grown at 37 °C with shaking at 280 rpm until the OD_{600} was ~0.6. Protein expression was induced by addition of 1 mM IPTG, followed by growth for an additional 4 h. Cells were harvested by centrifugation at 10,000*g* for 30 min. All steps after cell growth were carried out at 4 °C. The cell pellets from 6 L of growth were gently resuspended in 250 mL of 50 mM Tris-HCl (pH 7.5), 250 mM NaCl, and cell lysis was accomplished by sonication with 20 cycles of a 30 s pulse and 2 min rest at 75% power. The lysates were clarified by centrifugation at 31,000*g*, and the supernatants were loaded directly to a Ni-NTA (Qiagen) column equilibrated with lysis buffer plus 20 mM imidazole. The column was washed with 6 volumes of the same buffer, and protein was eluted with 250 mM imidazole. Protein-containing fractions were checked by SDS-PAGE and combined prior to dialysis against 50 mM potassium phosphate with 5 mM β-mercaptoethanol and 50% (v/v) glycerol. Dialyzed enzymes were stored at −20 °C and were active for at least 3 months. Yields ranged from 10−150 mg of purified protein per liter of culture depending on the enzyme, but different preparations of each enzyme were generally consistent (see Supplementary Table 1 and Supplementary Figure 1).

Enzymatic Assays. Enzymatic activity is reported in terms of units (U), where 1 U is the amount of enzyme required to convert 1 μmol min^{-1} of substrate into product, and the specific activity is reported as U mg^{-1}. Enzymatic activities were deter-

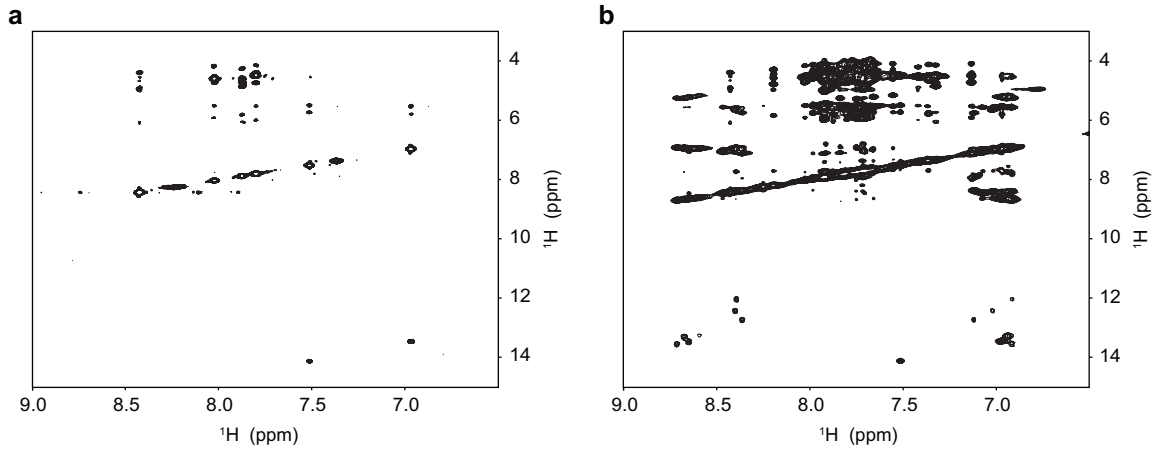

Figure 8. Spectra of TAR RNA. a) ^{13}C-edited and b) homonuclear NOESY (T_{mix} = 250 ms) spectra of TAR RNA uniformly labeled with ^{15}N-labeled guanosine and adenosine labeled with ^{13}C at positions 2 and 8.

mined only for *guaB, guaA, purB, purA, purF*, and *purD* in Figure 1, panel b, and for all enzymes in Figure 1, panels a and c except *folD* and *glyA* by coupling the reaction to consumption of ATP, which is monitored by the change in A_{340} due to the action of lactate dehydrogenase on ADP and NADH (*17*). To assay inorganic pyrophosphatase, the phosphate detection method of Michelson was used (*42*). When substrates were not available, the amount of enzyme was estimated empirically, using an assumed specific activity of 1 U mg^{-1}. Table 1 shows the amount of each enzyme added in units or milligrams for each synthesis.

Nucleotide Synthesis. *Synthesis of 2,8-^{13}C-ATP (**1**).* Stoichiometric substrates: 212 mg (1.2 mmol) glucose, 1 g (18.8 mmol) NH_4Cl, 687 mg (4.7 mmol) glutamine, 500 mg (4.7 mmol) $^{13}C_3$-serine, 235 mg (2.35 mmol) $KHCO_3$. Fuel reagents: 2.12 g (9.4 mmol) α-KG, 7.7 g (23.5 mmol) creatine phosphate. Catalytic cofactors: 6.43 mg (0.012 mmol) ATP, 6.6 mg (0.012 mmol) GTP, 8.8 mg (0.012 mmol) $NADP^+$, 68 mg (0.12 mmol) THF, 38 mg (0.24 mmol) fumarate. Substrates and cofactors were combined in 50 mM KH_2PO_4/K_2HPO_4, pH 7.6, 20 mM $MgCl_2$, 20 mM DTT, 100 μg mL^{-1} ampicillin, 50 μg mL^{-1} kanamycin. Enzymes were added according to Table 1 (**1**), giving a final volume of 120 mL. HPLC chromatograms of the reaction timecourse are included in Supplementary Figure 2.

*Synthesis of U-^{15}N-GTP (**2**).* Stoichiometric substrates: 212 mg (1.2 mmol) glucose, 1.27 g (23.5 mmol) $^{15}NH_4Cl$, 1.0 g (7 mmol) $^{15}N_{amide}$-glutamine, 500 mg (4.7 mmol) ^{15}N-serine, 235 mg (2.35 mmol) $KHCO_3$. Fuel reagents: 2.7 g (11.8 mmol) α-KG, 9.6 g (29 mmol) creatine phosphate. Catalytic cofactors: 6.43 mg (0.012 mmol) ATP, 64.3 mg (0.12 mmol) dATP, 8.8 mg (0.012 mmol) $NADP^+$, 8.4 mg (0.012 mmol) NAD^+, 68 mg (0.12 mmol) THF, 19 mg (0.12 mmol) fumarate. Substrates and cofactors were added to 50 mM KH_2PO_4/K_2HPO_4, pH 7.6, 20 mM $MgCl_2$, 20 mM DTT, 100 μg mL^{-1} ampicillin, 50 μg mL^{-1} kanamycin. Enzymes were added according to Table 1 (**2**), giving a final volume of 120 mL.

*Synthesis of U-^{13}C,^{15}N-GTP (**3**).* Stoichiometric substrates: 93 mg (0.5 mmol) $^{13}C_6$-glucose, 605 mg (1.1 mmol) $^{15}NH_4Cl$, 165 mg (1.5 mmol) ^{13}C,^{15}N- serine, 85 mg (1 mmol) $NaH^{13}CO_3$. Fuel reagents: 1.13 g (5 mmol) α-KG, 5.25 g (16 mmol) creatine phosphate. Catalytic cofactors: 2.68 mg (0.005 mmol) ATP, 26.8 mg (0.050 mmol) dATP, 3.7 mg (0.005 mmol) $NADP^+$, 3.5 mg (0.005 mmol) NAD^+, 5 mg (0.0085 mmol) THF, 8 mg (0.05 mmol) fumarate. Substrates and cofactors were added to 25 mM KH_2PO_4/K_2HPO_4, pH 7.6, 10 mM $MgCl_2$, 10 mM DTT, 50 μg mL^{-1} ampicillin, and 25 μg mL^{-1} kanamycin and flushed thoroughly with argon. Enzymes were added according to Table 1 (**3**), giving a final volume of 100 mL. Argon was gently bubbled again, and the glass flask was sealed. An equal amount of additional creatine phosphate was added during this reaction because of increased consumption of (d)ATP by *glnA*.

*Synthesis of U-^{13}C-GTP (**4**).* Stoichiometric substrates: 93 mg (0.5 mmol) $^{13}C_6$-glucose, 594 mg (1.1 mmol) NH_4Cl, 441 mg (3 mmol) glutamine, 163.5 mg (1.5 mmol) ^{13}C-serine, 85 mg (1 mmol) $NaH^{13}CO_3$. Fuel reagents: 1.13 g (5 mmol) α-KG, 4.6 g (14 mmol) creatine phosphate. Catalytic cofactors: 2.68 mg (0.005 mmol) ATP, 26.8 mg (0.050 mmol) dATP, 3.7 mg (0.005 mmol) $NADP^+$, 3.5 mg (0.005 mmol) NAD^+, 5 mg (0.0085 mmol) THF, 8 mg (0.05 mmol) fumarate. Substrates and cofactors were added to 25 mM KH_2PO_4/K_2HPO_4, pH 7.6, 10 mM $MgCl_2$, 10 mM DTT, 50 μg mL^{-1} ampicillin, 25 μg mL^{-1} kanamycin and flushed thoroughly with argon. Enzymes were added according to Table 1 (**4**), giving a final volume of 100 mL. Argon was gently bubbled again, and the glass flask was sealed.

ATP/GTP formation was monitored by HPLC using a Vydac nucleotide ion exchange column (250 mm × 4.6 mm), using a linear gradient of Buffer A (25 mM Na_2HPO_4/NaH_2PO_4 (1:1) adjusted to pH 2.8 with acetic acid) and Bufffer B (125 mM Na_2HPO_4/NaH_2PO_4 (1:1) adjusted to pH 2.9 with acetic acid) over 30 min at a flow rate of 2 mL/min. ATP/GTP formation was monitored at 260 nm.

Nucleotide Purification. The reaction was sterilized by filtration through a 0.2 μm filter, ammonium bicarbonate was added to a final concentration of 0.5 M, and the pH was adjusted to 9.65 with ammonium hydroxide. The solution was filtered again and loaded to a 15 g column of Affigel 601 (Biorad) boronate affinity resin equilibrated with 0.5 M ammonium bicarbonate pH 9.65 at RT. The column was washed with the same buffer, and nucleotides were eluted with water acidified with CO_2. The products were verified by HPLC, NMR and mass spectrometry. Final HPLC and mass spectrometry data for nucleotides **1**−**4** are given in Supporting Information.

RNA Synthesis. HIV-2 TAR RNA (5′GGCCAGAUUGAGCCUGGGAGCUCUCUGGCC3′) was synthesized by *in vitro* transcription with T7 RNA polymerase using a mixture of unlabeled UTP and CTP from Sigma and $^{13}C_{2,8}$-ATP and U-^{15}N-GTP. RNA was synthesized in a 20-mL reaction under optimized conditions: 21 mM total NTPs (5.25 mM each), 40 mM Tris HCl (pH 8.1), 0.1 mM sper-

midine, 10 mM DTT, 28 mM $MgCl_2$, 0.001% Triton X-100, 80 mg mL^{-1} poly(ethylene glycol) (8000 MW), 300 nM each DNA strand (Invitrogen), and 0.65 mg mL^{-1} T7 RNA polymerase, incubated at 37 °C for 4 h. The RNA was purified on denaturing 20% polyacrylamide gels, electro-eluted and desalted, lyophilized, and diluted in 10 mM sodium phosphate (pH 6.5), 150 mM NaCl, 10% D_2O for recording NMR spectra.

NMR Experiments. The spectral benefits of specifically labeling the adenosine and guanosine residues with ^{13}C and ^{15}N isotopes were assessed with two-dimensional correlation spectroscopy. One- and two-bond coupled $^1H,^{15}N$-HSQC correlation experiments were collected using INEPT transfer delay times (2Δ) of 5 and 42 μs, respectively (*43*). Spectra were recorded on a 500 MHz Bruker Avance spectrometer equipped with a 5 mm TXI-HCN triple resonance probe with a *z*-axis gradient. Homonuclear and isotope-edited NOESY experiments (T_{mix} = 250 ms) were collected on a 900 MHz Bruker Avance spectrometer equipped with a triple resonance 5 mm TXI-HCN probe with triple-axis gradients. Water suppression was achieved through the use of flip-back pulses and the Watergate scheme (*44*, *45*). $^1H,^{13}C$-HSQC spectra were collected using echo/antiecho gradient selection. Spectra were collected at 10 °C, referenced to 2,2-dimethyl-2-silapentane-5-sulfonate, processed with NMRPipe, and viewed in NMRDraw (*46*).

Acknowledgment: This work was supported by the National Institutes of Health (GM-74330). We thank Fabio Agnelli for collection of ^{13}C NMR spectra in Supporting Information and for preparations of glucokinase and glucose-6-phosphate dehydrogenase used in the syntheses.

Supporting Information Available: This material is free of charge *via* the Internet.

REFERENCES

1. Melnick, J. S., Sprinz, K. I., Reddick, J. J., Kinsland, C., and Begley, T. P. (2003) An efficient enzymatic synthesis of thiamin pyrophosphate, *Bioorg. Med. Chem. Lett. 13*, 4139–4141.
2. Rocha-Uribe, A., and Hernandez, E. (2004) Solvent-free enzymatic synthesis of structured lipids containing CLA from coconut oil and tricaprylin, *J. Am. Oil Chem. Soc. 81*, 685–689.
3. Zhu, D. M., Mukherjee, C., and Hua, L. (2005) "Green" synthesis of important pharmaceutical building blocks: enzymatic access to enantiomerically pure α-chloroalcohols, *Tetrahedron: Asymmetry 16*, 3275–3278.
4. van den Heuvel, R. H. H., Fraaije, M. W., Laane, C., and van Berkel, W. J. H. (2001) Enzymatic synthesis of vanillin, *J. Agric. Food Chem. 49*, 2954–2958.
5. Ohdan, K., Fujii, K., Yanase, M., Takaha, T., and Kuriki, T. (2007) Phosphorylase coupling as a tool to convert cellobiose into amylose, *J. Biotechnol. 127*, 496–502.
6. Koreishi, M., Tani, K., Ise, Y., Imanaka, H., Imamura, K., and Nakanishi, K. (2007) Enzymatic synthesis of β-lactam antibiotics and *N*-fatty-acylated amino compounds by the acyl-transfer reaction catalyzed by penicillin V acylase from *Streptomyces mobaraensis*, *Biosci., Biotechnol., Biochem. 71*, 1582–1586.
7. Huang, K. T., Wu, B. C., Lin, C. C., Luo, S. C., Chen, C., Wong, C. H., and Lin, C. C. (2006) Multi-enzyme one-pot strategy for the synthesis of sialyl Lewis X-containing PSGL-1 glycopeptide, *Carbohydr. Res. 341*, 2151–5.
8. Sugiyama, M., Hong, Z., Liang, P. H., Dean, S. M., Whalen, L. J., Greenberg, W. A., and Wong, C. H. (2007) D-Fructose-6-phosphate aldolase-catalyzed one-pot synthesis of iminocyclitols, *J. Am. Chem. Soc. 129*, 14811–7.
9. Yamaguchi, S., Komeda, H., and Asano, Y. (2007) New enzymatic method of chiral amino acid synthesis by dynamic kinetic resolution of amino acid amides: Use of stereoselective amino acid amidases in the presence of α-amino-ε-caprolactam racemase, *Appl. Environ. Microbiol. 73*, 5370–5373.
10. Roessner, C. A., Spencer, J. B., Stolowich, N. J., Wang, J., Nayar, G. P., Santander, P. J., Pichon, C., Min, C., Holderman, M. T., and Scott, A. I. (1994) Genetically engineered synthesis of precorrin-6x and the complete corrinoid, hydrogenobyrinic acid, an advanced precursor of vitamin B12, *Chem Biol 1*, 119–24.
11. Kajiwara, Y., Santander, P. J., Roessner, C. A., Perez, L. M., and Scott, A. I. (2006) Genetically engineered synthesis and structural characterization of cobalt-precorrin 5A and 5B, two new intermediates on the anaerobic pathway to vitamin B-12: Definition of the roles of the CbiF and CbiG enzymes, *J. Am. Chem. Soc. 128*, 9971–9978.
12. Scott, A. I. (1994) Genetically-engineered synthesis of natural products, *J. Nat. Prod. 57*, 557–573.
13. Kuberan, B., Lech, M. Z., Beeler, D. L., Wu, Z. L., and Rosenberg, R. D. (2003) Enzymatic synthesis of antithrombin III-binding heparan sulfate pentasaccharide, *Nat. Biotechnol. 21*, 1343–6.
14. Cheng, Q., Xiang, L., Izumikawa, M., Meluzzi, D., and Moore, B. S. (2007) Enzymatic total synthesis of enterocin polyketides, *Nat. Chem. Biol. 3*, 557–8.
15. Tolbert, T. J., and Williamson, J. R. (1996) Preparation of specifically deuterated RNA for NMR studies using a combination of chemical and enzymatic synthesis, *J. Am. Chem. Soc. 118*, 7929–7940.
16. Tolbert, T. J., and Williamson, J. R. (1997) Preparation of specifically deuterated and C-13-labeled RNA for NMR studies using enzymatic synthesis, *J. Am. Chem. Soc. 119*, 12100–12108.
17. Scott, L. G., Tolbert, T. J., and Williamson, J. R. (2000) Preparation of specifically H-2- and C-13-labeled ribonucleotides, *RNA–Ligand Interact., Part A 317*, 18–38.
18. Batey, R. T., Inada, M., Kujawinski, E., Puglisi, J. D., and Williamson, J. R. (1992) Preparation of isotopically labeled ribonucleotides for multidimensional NMR-spectroscopy of RNA, *Nucleic Acids Res. 20*, 4515–4523.
19. Nikonowicz, E. P., Sirr, A., Legault, P., Jucker, F. M., Baer, L. M., and Pardi, A. (1992) Preparation of C-13 and N-15 labeled RNAs for heteronuclear multidimensional NMR-studies, *Nucleic Acids Res. 20*, 4507–4513.
20. Batey, R. T., Battiste, J. L., and Williamson, J. R. (1995) Preparation of isotopically enriched RNAs for heteronuclear NMR, *Methods Enzymol. 261*, 300–22.
21. Cromsigt, J., Schleucher, J., Gustafsson, T., Kihlberg, J., and Wijmenga, S. (2002) Preparation of partially H-2/C-13-labelled RNA for NMR studies. Stereo-specific deuteration of the H5′′ in nucleotides, *Nucleic Acids Res. 30*, 1639–1645.
22. LaFrancois, C. J., Fujimoto, J., and Sowers, L. C. (1999) Synthesis and utilization of C-13(8)-enriched purines, *Nucleosides Nucleotides Nucleic Acids 18*, 23–37.
23. SantaLucia, J., Shen, L. X., Cai, Z. P., Lewis, H., and Tinoco, I. (1995) Synthesis and NMR of RNA with selective isotopic enrichment in the bases, *Nucleic Acids Res. 23*, 4913–4921.
24. Davis, J. H., Tonelli, M., Scott, L. G., Jaeger, L., Williamson, J. R., and Butcher, S. E. (2005) RNA helical packing in solution: NMR structure of a 30 kDa GAAA tetraloop-receptor complex, *J. Mol. Biol. 351*, 371–82.
25. Jiang, F., Patel, D. J., Zhang, X., Zhao, H., and Jones, R. A. (1997) Specific labeling approaches to guanine and adenine imino and amino proton assignments in the AMP-RNA aptamer complex, *J. Biomol. NMR 9*, 55–62.
26. Gmeiner, W. H. A. P., and Dale, C. (1988) An efficient synthesis of [8-13C]adenine, *J. Org. Chem. 53*, 1322–1323.
27. Barrio, M. D., Scopes, D. I., Holtwick, J. B., and Leonard, N. J. (1981) Syntheses of all singly labeled [N]adenines: Mass spectral fragmentation of adenine, *Proc. Natl. Acad. Sci. U.S.A. 78*, 3986–3988.

28. Abad, J. L., Gaffney, B. L., and Jones, R. A. (1999) ^{15}N-Multilabeled adenine and guanine nucleosides. Syntheses of [1,3,NH_2-$^{15}N_3$]- and [2-^{13}C-1,3,NH_2-$^{15}N_3$]-labeled adenosine, guanosine, 2′-deoxyadenosine, and 2′-deoxyguanosine, *J. Org. Chem. 64*, 6575–6582.
29. Zhao, H., Pagano, A. R., Weimin, W., Shallop, A., Gaffney, B. L., and Jones, R. A. (1997) Use of a ^{13}C atom to differentiate two ^{15}N-labeled nucleosides. Synthesis of [$^{15}NH_2$]-adenosine, [1,NH_2-$^{15}N_2$]- and [2-^{13}C-1,NH_2-$^{15}N_2$]-guanosine, and [1,7,NH_2-$^{15}N_3$]- and [2-^{13}C-1,7,NH_2-$^{15}N_3$]-2′-deoxyguanosine, *J. Org. Chem. 62*, 7832–7835.
30. Bouhss, A., Sakamoto, H., Palibroda, N., Chiriac, M., Sarfati, R., Smith, J. M., Craescu, C. T., and Barzu, O. (1995) Enzymatic-synthesis of guanine-nucleotides labeled with N-15 at the 2-amino group of the purine ring, *Anal. Biochem. 225*, 18–23.
31. Lagoja, I. M., and Herdewijn, P. (2002) Chemical synthesis of C-13 and N-15 labeled nucleosides, *Synthesis (Stuttgart)* 301–314.
32. Crans, D. C., Kazlauskas, R. J., Hirschbein, B. L., Wong, C. H., Abril, O., and Whitesides, G. M. (1987) Enzymatic regeneration of adenosine 5′-triphosphate: acetyl phosphate, phosphoenolpyruvate, methoxycarbonyl phosphate, dihydroxyacetone phosphate, 5-phospho-α-D-ribosyl pyrophosphate, uridine-5′-diphosphoglucose, *Methods Enzymol. 136*, 263–80.
33. Chenault, H. K., and Whitesides, G. M. (1987) Regeneration of nicotinamide cofactors for use in organic synthesis, *Appl. Biochem. Biotechnol. 14*, 147–97.
34. Zhao, H. M., and van der Donk, W. A. (2003) Regeneration of cofactors for use in biocatallysis, *Curr. Opin. Biotechnol. 14*, 583–589.
35. Chenault, H. K., Simon, E. S., and Whitesides, G. M. (1988) Cofactor regeneration for enzyme-catalysed synthesis, *Biotechnol. Genet. Eng. Rev. 6*, 221–70.
36. Hennig, M., Scott, L. G., Sperling, E., Bermel, W., and Williamson, J. R. (2007) Synthesis of 5-fluoropyrimidine nucleotides as sensitive NMR probes of RNA structure, *J. Am. Chem. Soc. 129*, 14911–21.
37. Scott, L. G., Geierstanger, B. H., Williamson, J. R., and Hennig, M. (2004) Enzymatic synthesis and ^{19}F NMR studies of 2-fluoroadenine-substituted RNA, *J. Am. Chem. Soc. 126*, 11776–7.
38. Kappock, T. J., Ealick, S. E., and Stubbe, J. (2000) Modular evolution of the purine biosynthetic pathway, *Curr. Opin. Chem. Biol. 4*, 567–572.
39. Gross, A., Abril, O., Lewis, J. M., Geresh, S., and Whitesides, G. M. (1983) Practical synthesis of 5-phospho-D-ribosyl α-1-pyrophosphate (PRPP): enzymatic routes from ribose 5-phosphate or ribose, *J. Am. Chem. Soc. 105*, 7428–7435.
40. Chen, L. H., Babbitt, P. C., Vasquez, J. R., West, B. L., and Kenyon, G. L. (1991) Cloning and expression of functional rabbit muscle creatine kinase in Escherichia coli. Addressing the problem of micro-heterogeneity, *J. Biol. Chem. 266*, 12053–7.
41. Luo, S., Kim, G., and Levine, R. L. (2005) Mutation of the adenylylated tyrosine of glutamine synthetase alters its catalytic properties, *Biochemistry 44*, 9441–6.
42. MIchelson, O. B. (1957) Photometric determination of phosphorous as molybdovanadophosphoric acid, *Anal. Chem. 29*, 60–62.
43. Sklenar, V., Peterson, R. D., Rejante, M. R., and Feigon, J. (1994) Correlation of nucleotide base and sugar protons in a N-15-labeled HIV-1 RNA oligonulceotide by H-1-N-15 HSQC experiments, *J. Biomol. NMR 4*, 117–122.
44. Grzesiek, S., and Bax, A. (1993) The importance of not saturating H_2O in protein NMR. Application to sensitivity enhancement and NOE measurements, *J. Am. Chem. Soc. 115*, 12593–12594.
45. Piotto, M., Saudek, V., and Sklenar, V. (1992) Gradient-tailored excitation for single-quantum NMR spectroscopy of aqueous solutions, *J. Biomol. NMR 2*, 661–665.
46. Delaglio, F., Grzesiek, S., Vuister, G. W., Zhu, G., Pfeifer, J., and Bax, A. (1995) NMRPipe: a multidimensional spectral processing system based on UNIX pipes, *J. Biomol. NMR 6*, 277–93.
47. Mueller, E. J., Meyer, E., Rudolph, J., Davisson, V. J., and Stubbe, J. (1994) N^5-Carboxyaminoimidazole ribonucleotide: evidence for a new intermediate and two new enzymatic activities in the *de novo* purine biosynthetic pathway of *Escherichia coli*, *Biochemistry 33*, 2269–2278.